Robustness to water and temperature, and activation energies of metakaolin-based geopolymer and alkali-activated slag binders

Hugo Lahalle, Virginie Benavent, Vincent Trincal, Thomas Wattez, Raphaël Bucher, Martin Cyr

▶ **To cite this version:**

Hugo Lahalle, Virginie Benavent, Vincent Trincal, Thomas Wattez, Raphaël Bucher, et al.. Robustness to water and temperature, and activation energies of metakaolin-based geopolymer and alkali-activated slag binders. Construction and Building Materials, 2021, 300, pp.124066. 10.1016/j.conbuildmat.2021.124066 . hal-03346130

HAL Id: hal-03346130
https://hal.insa-toulouse.fr/hal-03346130

Submitted on 2 Aug 2023

HAL is a multi-disciplinary open access archive for the deposit and dissemination of scientific research documents, whether they are published or not. The documents may come from teaching and research institutions in France or abroad, or from public or private research centers.

L'archive ouverte pluridisciplinaire **HAL**, est destinée au dépôt et à la diffusion de documents scientifiques de niveau recherche, publiés ou non, émanant des établissements d'enseignement et de recherche français ou étrangers, des laboratoires publics ou privés.

Distributed under a Creative Commons Attribution - NonCommercial 4.0 International License

Version of Record: https://www.sciencedirect.com/science/article/pii/S0950061821018262
Manuscript_c4cb157864cee249d1a7b82396bd713e

Robustness to water and temperature, and activation energies of metakaolin-based geopolymer and alkali-activated slag binders

Hugo LAHALLE[1], Virginie BENAVENT[1], Vincent TRINCAL[1], Thomas WATTEZ[2], Raphaël BUCHER[3], Martin CYR[1,*]

1. Université de Toulouse, UPS, INSA, LMDC (Laboratoire Matériaux et Durabilité des Constructions de Toulouse), 135 Avenue de Rangueil, 31077, Toulouse cedex 04, France.
2. Ecocem Materials, 4 Place Louis Armand, 75012 Paris, France.
3. ARGECO Développement, Fumel, France.

Abstract:

The aim of this paper is to evaluate the properties of four alkali-activated materials subjected to precasting and in situ concreting conditions: fluctuations in water content (± 5%) and in temperature (10°C, 20°C, 30°C). The initial slump and compressive strengths at 1, 2, 7, 28 and 90 days of a metakaolin-based geopolymer, and of sodium silicate-activated slag, sodium metasilicate-activated slag and sodium carbonate-activated slag mortars were determined, then compared to the properties of an ordinary Portland cement mortar (CEM I). A total of 50 mortars were cast for the five formulations studied and the different conditions. This paper reports that alkali-activated materials are as robust as CEM I in precasting and in situ concreting conditions. However, some adjustments should be made to offset the low reactivity in cold weather, such as hot water or hot curing, or reducing the water/binder ratio. The apparent activation energies were determined for the five pastes to explain these observations.

Keywords: metakaolin and slag alkali-activated binders, geopolymer, robustness, temperature, water content, energy activation

* **Corresponding author:** cyr@insa-toulouse.fr

© 2021 published by Elsevier. This manuscript is made available under the CC BY NC user license
https://creativecommons.org/licenses/by-nc/4.0/

1 Introduction

Alkali-activated binders have been widely considered as clinker-free binders that may offer prospects to replace Portland cement in some applications, in order to reduce carbon emissions of construction industry. Alkali-activated binders, if produced using locally available raw materials (fly ashes, calcined clays, slags), could be effective components of the future toolkit of sustainable construction materials. These materials could be used as concrete-based building materials for high volume applications in reinforced concrete, plain concrete, precast concrete components, mortars, grouts and renders, foamed and lightweight concretes, matrices for the immobilization of toxic and nuclear wastes, in precast as well as in situ concreting [1], [2]. They have already been used for large-scale applications worldwide, including in the construction of an airport in Australia [3], longstanding application and standardization in Ukraine and Russia [4], [5], and a building in China [6].

Alkali-activated binders are made by mixing solid aluminosilicate precursors, such as fly ash and metakaolin (low-calcium precursors), or blast furnace slag (high-calcium precursor), with alkali-activators (MOH, $M_2O.rSiO_2$, M_2CO_3, M_2SO_4, where M is often either Na or K). Depending on the nature and characteristics of the precursors and the activators, different setting kinetics, properties and mineralogy are observed [2], [7], [8]. They are generally amorphous materials with some crystalline phases. Metakaolin-based geopolymer consists of a 3D-aluminosilicate network with alkali cations playing the role of charge-balancing ions [9]. Sodium silicate-activated slag and sodium carbonate-activated slag contain hydrates, mainly C-(N-)A-S-H and hydrotalcite-type phases [10]–[13]. Metakaolin-based geopolymer and sodium silicate-activated slag set fast with very high and moderate compressive strengths, respectively, at early age [14]–[16], while the sodium carbonate-activated slag has a prolonged hardening process related to the slow development of alkalinity required to initiate the dissolution of slag, with low compressive strengths at early age (up to 3-4 days) [14], [16]. It is for this reason that there is not a universal mix design procedure for alkali-activated materials but one for each precursor. An optimization is needed [1], [17].

Many studies have looked into the influence of the formulation [16], [18]–[25], the water content [25], [26], and the curing period and temperature [16], [20], [27]–[31] on the binder properties, generally for specific formulations (geopolymer, sodium silicate or carbonate-activated slag). However, to the best of our knowledge, only very few papers have dealt with their robustness in comparison with Portland cement. Provis [1] considers the robustness of the technology for alkali-activated materials, discussing what is possible and what needs further development. In a second paper, Provis et al. [15] report an inter-laboratory study including 15 laboratories to determine the reproducibility of five alkali-activated materials: two sodium silicate-activated slag materials, two fly ash-based geopolymers and one metakaolin-based geopolymer. The round-robin test outcomes showed that each participating laboratory was able to reproducibly produce alkali-activated concretes, the inter-laboratory deviations being broadly consistent with the expectations for Portland cement-based concretes. Typically, variations of 20% to 30% in the compressive strengths were observed for alkali-activated slag concretes and less than 20% for metakaolin-based geopolymer concrete, while variations of up to 50% have been reported for Portland cement concrete [32]. The within-laboratory reproducibility of the test results was very good, with no more than 10% spread across replicates in any given laboratory (comparable to Portland cement). The difference was mostly attributed to the compatibility of the binder with aggregates, since each laboratory used its own aggregates, potentially differing in mineralogy and characteristics.

Thus, the next step for considering the use of alkali-activated materials as replacements for conventional cements requires studies of their sensitivity to water content and temperature in the conditions that might be encountered for precast and cast-in-situ concrete. In that respect, the

robustness to water content (± 5% of water) and possible outdoor temperature in a moderate climate (10°C for the winter period and 30°C for summer) was determined for four alkali-binders: one metakaolin-based geopolymer, two sodium silicate-activated slags and one sodium carbonate-activated slag, and then compared to one Portland cement (CEM I). The aim of this paper is to provide a better understanding of the fresh and hardened state properties (slump and compressive strengths) of alkali-activated materials when they are handled and used for civil engineering applications.

One way of addressing the dependence of cementitious materials on temperature is to consider their apparent activation energy. That is why, for the first time, the apparent activation energies were determined simultaneously for four different alkali-activated binders, alongside that of CEM I, by isothermal calorimetry at 12°C, 20°C and 30°C. Previous studies have generally focused on Portland cement and Blended cement [33]–[39] or on one specific alkali-activated binder: sodium silicate activated slag [40]–[43] or metakaolin, or pozzolan geopolymers [44]–[47]. Temperature and experimental techniques have varied depending on the authors (adiabatic or isothermal calorimetry, compressive strength, rheological measurements with viscosity models, X-ray total scattering measurements and pair distribution function, PDF).

2 Experimental methodology

2.1 Materials

The alkali-activated materials were prepared from two precursors: Argicem® metakaolin manufactured by ARGECO Développement at Fumel, France, and ground-granulated blast-furnace slag (GGBS) manufactured by ECOCEM France at Fos-sur-Mer, France. The metakaolin was obtained by flash calcination at 750°C for a few tenths of second. It is a ground material with a density of 2.59 g/cm^3 and a specific surface area of 17 m^2/g (BET). The GGBS used had a density of 2.93 g/cm^3, a Blaine's specific surface area of 4633 cm^2/g and a 28-day activity index of 98% (NF EN 196-1). The GGBS was mainly amorphous, while the metakaolin comprised 47.1 ± 2.5% by weight of amorphous phase and a large proportion of quartz (42.3 ± 1.6 wt%), together with accessory minerals such as calcite, kaolinite, mullite and iron and titanium oxides. The compositions are given in Table 1 and Table 2.

Table 1: Metakaolin mineralogical composition estimated by Rietveld modelling on X-ray diffractograms.

Phases	Proportion (wt%)
Amorphous	47.1 ± 2.5
Quartz	42.3 ± 1.6
Illite	3.5 ± 0.5
Mullite	3.1 ± 0.4
Anatase	1.5 ± 0.1
Calcite	1.0 ± 0.1
Hematite	0.9 ± 0.1
Rutile	0.3 ± 0.1

Table 2: Chemical composition of raw materials obtained with X-ray fluorescence analyses.

Raw materials	SiO_2 (wt%)	Al_2O_3 (wt%)	CaO (wt%)	Fe_2O_3 (wt%)	Na_2O (wt%)	K_2O (wt%)	TiO_2 (wt%)	MgO (wt%)	MnO (wt%)	LOI (wt%)	Total (wt%)
Metakaolin	68.2	23.4	0.7	3.6	0.2	0.2	1.2	1.2	0.0	1.3	100

GGBS	37.3	11.9	42.8	0.5	0.2	0.3	0.5	6.3	0.1	0.0	100
CEM I 52.5 N	20.1	5.3	64.3	3.4	0.3	0.7	0.0	0.8	0.0	1.8	96.7

CEM I 52.5 N CE CP2 NF from EQIOM (Lumbres, France), was used as the reference material for this study. It is composed of 92 wt% of clinker, 3 wt% of limestone filler, and 5 wt% of gypsum as a set regulator. Its Blaine's specific surface area is 4400 cm^2/g and its density is 3.09 g/cm^3. The clinker was composed of 61% C_3S, 19.3% C2S 8.6% C_3A, and 11.1% C_4AF, in mass percentage. Mechanical strengths were estimated by the supplier at 24 MPa, 38 MPa and 62 MPa after 1, 2 and 28 days, respectively (standardized mortar with water to cement ratio of 0.50).

Five types of mortars and pastes were prepared: a geopolymer, two sodium silicate-activated slag materials, a sodium carbonate-activated slag and one Portland cement (CEM I). Three activators were used for alkali-activated materials:

- a commercial sodium silicate solution, Betol 47T, from WOELLNER containing 55.5% by weight of water and 44.5% of activator with an SiO_2 to Na_2O mass ratio of 1.7, i.e. 27.5% of SiO_2 and 16.9% of Na_2O.
- a sodium silicate powder (sodium metasilicates: Na_2SiO_3, 50.7% Na_2O, 49.3% SiO_2) from SILMACO, with a density of 0.99 g/cm^3 (purity > 95%).
- a light sodium-carbonate (Na_2CO_3) from SOLVAY with a density of 2.53 g/cm^3 (purity > 99%).

Standard sand from Société Nouvelle du Littoral, composed of crystallized quartz and with a grain size distribution below 2 mm (CEN EN 196-1; ISO 679: 2009), and tap water from the city of Toulouse (France) were also used for mortar preparation.

2.2 Mortar and paste mix design, curing and testing methodology

The mortar mixtures were made in a standardized mixer (Automix Control®) according to the standard protocol NF EN 196-1 (60 seconds at 140 ± 5 rpm with sand addition after 30 seconds, 30 seconds at 285 ± 10 rpm, 90 second pause, 60 seconds at 285 ± 10 rpm), then poured at 20°C into 4x4x16 cm^3 polystyrene moulds. The test pieces were cast in two steps followed by 10 seconds of vibration on a vibrating table.

The five mortars (Table 3) were prepared with a sand to precursor/cement (slag, metakaolin or cement) mass ratio of 3. The water to binder (w/b, or cement: w/c) mass ratio was 0.4 for the four alkali-activated materials, and 0.5 for the Portland cement. The value of 0.5 was selected to facilitate the casting and vibration of the mortar bars and avoid the robustness results being influenced by mortar defects due to poor vibration; a dry mix was obtained with 0.4.

In the case of the four alkali-activated binders, binder was composed of precursor and dry activator. The activator content was chosen thanks to several preliminary tests done in the laboratory to reach at least 40 MPa at 28 days for a same water to binder ratio:

- The geopolymer consisted of a mix of metakaolin and Betol 47T (Geo). The amount of dry activator was fixed at 35.5 % of metakaolin. The formulation selected was based on precedent work [24].
- The sodium silicate-activated slag materials were prepared from a mix of slag and Betol 47T (10% of dry activator) (NaS-slag) or sodium metasilicates (8% of activator) (MS-slag). The decrease from 10 to 8% between silicate and metasilicate was due to a higher efficiency of the MS.
- The sodium carbonate-activated slag material consisted of a mix of slag and sodium-carbonate (NaC-slag).

The Portland cement was prepared using a CEM I 52.5 N CE CP2 NF (CEM I).

Table 3: Mix design of the five mortars tested (four alkali-activated materials and one Portland cement).

Raw materials (g)	CEM I	Geo	NaS-slag	MS-slag	NaC-slag
Metakaolin	-	450.0	-	-	-
Slag	-	-	450.0	450.0	450.0
CEM I	450.0	-	-	-	-
Betol 47T	-	354.9	101.3	-	-
Metasilicates	-	-	-	35.5	-
Na_2CO_3	-	-	-	-	45.0
Standard sand	1350.0	1350.0	1350.0	1350.0	1350.0
Tap water (g)	225.0	46.2	141.8	194.4	198.0
w/b or w/c	0.5	0.4	0.4	0.4	0.4

In order to study the robustness of these five mortars, the following conditions were chosen:

- The sensitivity to the water content was measured by adding or removing 5% of water in mass from the initial mix (Table 3). In the case of the four alkali-activated mortars, this implied w/b ratios of 0.380 and 0.420. In the case of the CEM I mortar, it implied w/b ratios of 0.475 and 0.525.

- The sensitivity to temperature was measured with three temperatures often encountered in France for winter (10°C), spring and autumn (20°C), and for summer (30°C). Although the weather may be colder (down to less than 0°C) or hotter (up to 40-45°C) during several days depending on the region and the season, the temperatures chosen here were 20°C ± 10°C, as construction workload often slows down outside these temperatures. The raw materials (powders, sand and liquids) were conditioned for 48 hours prior to casting at 10°C, 20°C, or 30°C. The mortars were prepared in a room, at the ambient temperature (20°C ± 3°C, 65% RH). Then the mortar bars were cured for 3 days in climatic chambers at the selected temperature (10°C, 20°C, or 30°C) before being stored at room temperature (20°C ± 3°C, 65% RH). These 3 days of curing were similar to those of control samples of casting for in situ concreting (samples generally left outside after casting and before being tested). The surface of the moulds was covered by a plastic sheet and plate to avoid excessive desiccation during the 3 days of curing. Mortar bars were also kept longer (28 days and 90 days) at 10°C in order to assess the influence of curing time on long-term compressive strength development.

The slump and the temperature of each mix were measured after mixing, with a small Abrams cone (height: 15 cm, Diameters: 5 cm and 10 cm) and a thermocouple, respectively.

The mortar bars (4x4x16 cm^3) were removed from their mould after 3 days of curing in the selected condition and sealed in plastic sheets at room temperature (20°C ± 3°C) to avoid desiccation. The compressive strengths were determined at 1, 2, 7, 28, and 90 days, repeating the measurement on 3 samples with standardized 3R presses following the standard protocol NF EN 196-1 (rate of load increase of 2400 ± 200 N/s). For the compressive strengths at 1 day and 2 days, only one mortar bar was removed from the mould, while the others were kept in it until 3 days of curing had elapsed. A mean value of compressive strength was determined on 3 samples, with a confidence interval of 95%.

Finally, five pastes were prepared as described in Table 3 without sand. They were made with a kitchen mixer according to the following protocol in five steps: liquid mixing for 2 min at slow speed, powder addition, mixing for 1 min at slow speed and 1 min at fast speed, stop for 30 sec and mixing

for 1 min at fast speed. The heats of reaction/hydration of the five pastes studied were measured over 10 days using a TAM Air isothermal calorimeter at 12°C, 20°C, and 30°C in order to determine the apparent activation energies of the four alkali-activated materials. The apparent activation energies were then compared to the ones measured on CEM I paste. The temperature of 12°C was selected rather than 10°C to avoid condensation within the calorimeter, which could lead to a deterioration of the device, due to the presence of liquid water (dew point at 12°C for the temperature (20°C) and relative humidity (50%) of the room).

The term "apparent activation energy" (E_a) was used for cementitious systems instead of using "activation energy" in order to take account of several simultaneous reactions that take place in these complex systems. Kada-Benameur et al. [39] showed that the apparent activation energy can be determined according to the degree of reaction (geopolymer) or hydration (cement and slag-activated materials) assuming that reaction/hydration kinetics follow the Arrhenius Equation (Eq. 1).

$$k = Ae^{\frac{-E_a}{RT}} \qquad (Eq.1)$$

k is the rate constant (sensitive to temperature), (sensitive to temperature),
T is the absolute temperature (in kelvins: K),
A is the pre-exponential factor, a constant for each chemical reaction,
E_a is the activation energy for the reaction (in the same units as RT, J/mol),
R is the universal gas constant (8.31 J/mol/K).

The apparent activation energy can then be determined according to the following equation (Eq. 2):

$$\frac{E_a}{RT} = -\ln(k) + \ln(A) \qquad (Eq.2)$$

The degree of reaction/hydration (α) can be defined (Eq. 3) by the ratio of cumulative heat released during measurement, Q(t), to the final quantity of heat released in the long term, Q_∞. Q_∞ is considered equal to the asymptotic value of the curves Q(t). In practice, Q(t) is obtained by plotting the curve Q = f(1/t) and the required asymptotic value Q_∞ is obtained by regression to X-axis at 1/t = 0.

$$\alpha(t) = \frac{\mathrm{Q(t)}}{\mathrm{Q}_\infty} \qquad (Eq.3)$$

In the case of one paste subjected to two different temperature histories (T_1, T_2), it is assumed that the two pastes will have the same degree of reaction/hydration at two different times (t_1, t_2).

$$\alpha_{T1}(t_1) = \alpha_{T2}(t_2) \qquad (Eq.4)$$

Thus, for the same degree of reaction/hydration, it can be assumed that the rate constant, k, is an inverse function of time (t_α), so the ratios of t_α values determined at different temperatures can be used instead of k to calculate E_a [44], [46]. Plotting $-\ln({}^{1}/_{t_\alpha})$ against $({}^{1}/_{RT})$, shows a linear relationship, with slope E_a (Eq. 5).

$$\frac{E_a}{RT} - \ln(A) = -\ln\left(\frac{1}{t_\alpha}\right) \qquad (Eq.5)$$

3 Results

3.1 Slump evolution for the five mortars

Table 4 gives the slump measurement for each mix depending on the water content and the temperature of the raw materials (powders + sand + liquids) before casting. The temperature measured after mixing is also specified for all the mixes. Despite an equal water to binder mass ratio of 0.4 for the four alkali-activated materials, the rheology of these four mixes presents significant differences. The slump is greater for geopolymer (Geo) and sodium silicate-activated slag (NaS-slag) than for metasilicate-activated slag (MS-slag) and carbonate-activated slag (NaC-slag). The use of a solution of sodium silicate, such as Betol 47T, enabled the mortars to flow but the geopolymer (Geo) and sodium silicate-activated slag (NaS-slag) were more viscous. In the case of geopolymer, the difference might also be partially explained by a higher volume of paste in the mortar: 607.9 g of binder (precursor + dry activator) for 1350 g of sand, while CEM I contained 450.0 g of binder and slag alkali-activated mortars 495.0 g of binder.

Table 4: Slumps and temperatures of the four alkali-activated materials and the Portland cement after mixing, according to the water content and temperature of the raw materials before casting.

	CEM I		Geo		NaS-slag		MS-slag		NaC-slag	
Conditions	**Slump (cm)**	**T_{mix} (°C)**	**Slump (cm)**	**T_{mix} (°C)**	**Slump (cm)**	**T_{mix} (°C)**	**Slump (cm)**	**T_{mix} (°C)**	**Slump (cm)**	**T_{mix} (°C)**
Reference [20°C]	0.5	23.9	7.5	24.7	8.5	22.9	0.5	26.8	0.5	25.9
Mixture -5% of H_2O	0.0	24.5	5.5	24.3	5.5	22.8	0.0	26.2	0.0	25.6
Mixture +5% of H_2O	1.8	24.4	10.0	24.1	11.0	22.0	2.0	25.6	6.5	25.8
Mixture with raw materials at 10°C	0.5	18.1	10.0	18.3	9.0	17.6	2.0	20.9	0.5	19.7
Mixture with raw materials at 30°C	0.5	28.4	7.0	28.9	3.5	26.6	0	29.3	3.5	29.6

For the five mortars (CEM I, Geo, NaS-Slag, MS-slag, NaC-slag), the slump increased/decreased with the water content (+5% H_2O/-5% H_2O). Altogether, MS-slag, NaC-slag and CEM I reference mortars presented low slump values, close to zero, in their initial mix design but proved to be impacted by 5% water addition in the same fashion as other mix designs (+2-3 cm of slump), with a more pronounced evolution in the case of the sodium silicate and carbonate activated slag mix (+6 cm of slump).

As regards the effect of the temperature of the raw materials, depending on the formulation, the temperature varied from 22.9°C to 26.8°C for the raw materials (powders + sand + liquids) stored at 20°C before mixing, while it varied from 17.6°C to 19.7°C and from 26.6°C to 29.6°C for the raw materials stored at 10°C and 30°C, respectively, for 48 hours before mixing. For each formulation, conditioning raw materials at 10°C or 30°C prior to mixing led to a difference of 4°C to 6°C within the mix in comparison with raw materials stored at 20°C. The temperature of the mix depended, not only on the initial storage conditions of the raw materials but also on exothermic reactions occurring in

the early stages of hydration. It has been demonstrated in several publications that the dissolution of metakaolin and the geopolymerization process are exothermic [48]–[51], as are the dissolution of cement and slag and the precipitation of C-S-H or C-(N-)A-S-H hydrates [13], [51]–[53]. Furthermore, it should be kept in mind that the temperature of the mix also depends on the specimen volume: the temperature will increase with the volume cast, as shown in the literature [54].

Regarding the slump tests, there was no relevant influence of temperature on CEM I mortar. For the three systems activated with silicates (NaS-slag, MS-slag, Geo), the slump was lower when the temperature was higher (30°C) and higher when the temperature was lower (10°C). For NaC-slag mortar, a higher slump was measured when the raw materials were stored at 30°C. This result might be explained by better dissolution of the activator (Na_2CO_3) [55].

3.2 Compressive strength of the five reference mortars

Figure 1 shows the compressive strengths measured for each of the reference samples kept in endogenous conditions at 20°C. The calculated confidence interval (CI) of 95% is also indicated for each mean value.

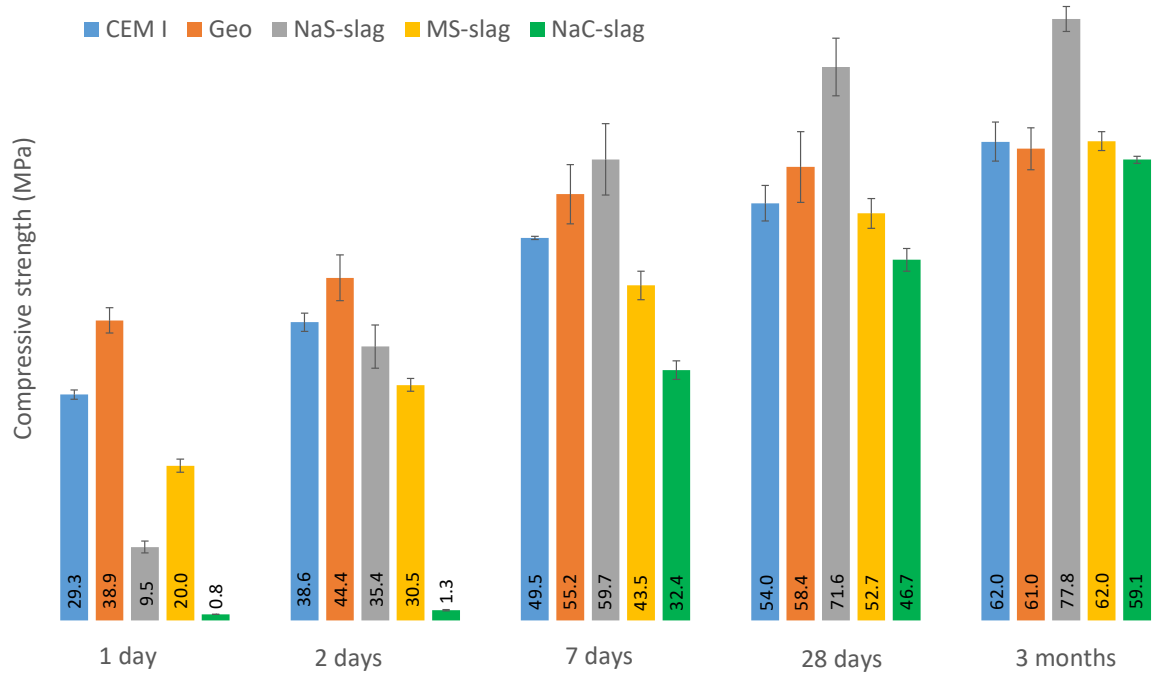

Figure 1: Evolution of compressive strengths over time for the five mortars studied.

All the mortars had high (29.3 MPa for CEM I, 38.9 MPa for Geo) or moderate (9.5 MPa for NaS-slag, 20 MPa for MS-slag) early age compressive strengths (1 day), except for NaC-slag mortar, which presented 0.8 MPa and 1.3 MPa at 1 and 2 days, respectively. This result could be explained by the low initial alkalinity of NaC-slag delaying the dissolution of slag.

All the mortars had compressive strengths above 45 MPa at 28 days. The mortar with the lowest mechanical strengths was NaC-slag mortar (46.7 MPa), and the mortar with the highest mechanical strength was NaS-slag mortar (71.6 MPa). The MS-slag mortar had lower 28-day compressive strength (52.7 MPa) than NaS-slag mortar since only 8% of activator (metasilicate powder) was used

instead of 10% of activator (dry content of Betol 47 T solution, see Table 3). Geo and CEM I mortar compressive strengths were respectively 58.6 MPa and 54 MPa at 28 days. At 90 days, the compressive strengths had continued to increase for all the mortars: 62.0 MPa for CEM I (+14.7%), 61.0 MPa for Geo (+4%), 77.8 MPa for NaS-slag (+8.7%), 62.0 MPa for MS-slag (+17.7%), and 59.1 MPa for NaC-slag (+27.7%). The strongest evolution was obtained for NaC-slag, which presented the slowest initial reaction rate.

3.3 Robustness of Portland cement (CEM I) mixtures

The CEM I mortar (w/c = 0.5, 20°C) prepared as a reference had a compressive strength of about 29.3 MPa to 62.0 MPa between 1 and 90 days. Figure 2 shows that increasing the water content by 5% obviously led to lower compressive strengths at all ages, but without significant effect of time (-13% to -19% between 1 and 90 days, without specific order). As regards the effect of raw material temperature for casting and the curing temperature, the early age and final compressive strengths were affected in different ways at 10°C and 30°C. Hot casting and curing temperature (30°C) yielded higher mechanical strengths at early age (35.1 MPa at 1 day, +20%) without significant influence on 28-day compressive strengths. However, lower compressive strengths at later age were obtained (-12% at 90 days) which could be explained by a limitation of the hydration of the cement over time due to its early reactivity [56], [57]. Cold casting and curing temperature (10°C) led to a strong decrease in mechanical strengths at 1 day (9.7 MPa, -66%), and 2 days (22.3 MPa, -42%). However, even though the compressive strengths were lower at early age - probably because of a lower initial reactivity [56]–[58] - after a longer maturing period (7, 28, and 90 days) in ambient temperature conditions, the mix had higher mechanical strengths. Compressive strengths of 40.6 MPa at 7 days, 55 MPa at 28 days, and 54.2 MPa at 90 days were measured for samples cured for three days at 30°C, while 54.5 MPa, 59.9 MPa and 69.3 MPa were measured for samples cured for three days at 10°C.

Longer curing times of 28 days and 90 days at 10°C led to higher compressive strengths: 66.0 MPa and 71.1 MPa, respectively. (+22% and +15% in comparison to CEM I reference mortar kept at 20°C, +10% and +3% in comparison to CEM I mortar kept for 3 days at 10°C and 25 days at 20°C). These results point out that longer cold curing time, possibly encountered during winter, might delay the development of early age properties but better performances would be attained at later ages (28, and 90 days). This will be discussed in Figure 9.

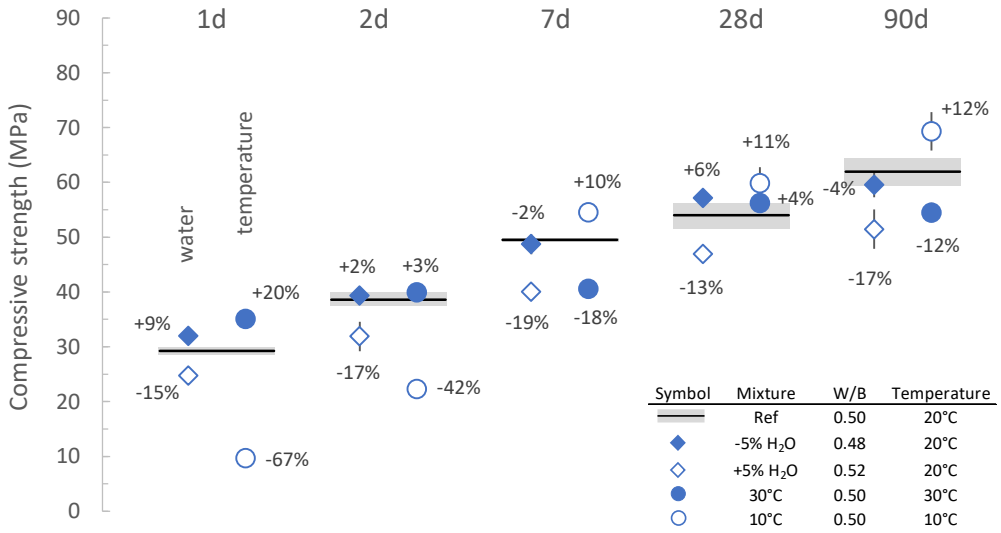

Figure 2: Evolution of compressive strengths in comparison to CEM I reference mortar depending on the water content (±5%) and temperature of the raw materials, at casting and during the first 3 days of curing.

3.4 Robustness of geopolymer (Geo) mixtures

The geopolymer mortar, in normal casting conditions (w/b = 0.4, 20°C), developed compressive strengths of 38.9 MPa to 61.0 MPa between 1 and 90 days. Figure 3 shows a lower dependence on water content in comparison to CEM I (-1% to -7% for 5% addition of water, without significant effect of time or specific order), and that reducing water content increased compressive strengths. Slight differences observed with respect to the reference geopolymer fell within the confidence interval of 95% (±3.8 MPa and ±4.5 MPa respectively). As for CEM I, it seemed that higher early compressive strengths were obtained for casting and curing at 30°C (+40%, 54.5 MPa and +23%, 54.6 MPa at 1 and 2 days respectively), and lower early mechanical strengths at 10°C (-100%, 0.0 MPa and -83%, 7.6 MPa at 1 and 2 days respectively). However, geopolymer early age properties were more dependent on casting and curing temperature. For instance, no compressive strength could be measured at 1 day for the sample cured at 10°C (the geopolymer mortar bar was still plastic and had not yet completely set), and only 7.6 MPa was observed at 2 days, which corresponds to a strength loss of more than 80% compared to the reference casting conditions. At later age (7, 28, and 90 days), the temperature of the raw materials and the curing temperature did not seem to have any strong influence on compressive strengths. Although the 90-day results showed the same trend as CEM I mortars, hot and cold casting and curing temperatures implied a decrease and an increase, respectively, of compressive strengths in the long run (55.2 MPa at 90 days for 30°C, and 66.3 MPa at 90 days for 10°C).

Longer curing times of 28 days and 90 days at 10°C yielded compressive strengths close (within the confidence interval of 95%) to those of the reference geopolymer mortar kept for 28 days at 20°C: 57.7 MPa (-2%) and 56.9 MPa (-7%), respectively (see Figure 9).

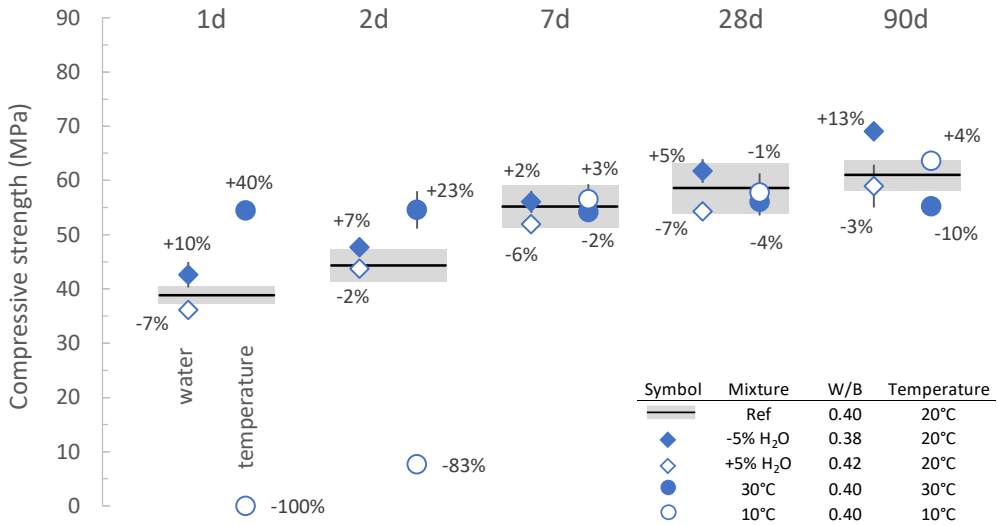

Figure 3: Evolution of compressive strengths in comparison to that of geopolymer reference mortar, depending on water content (±5%) and the temperature of raw materials and the 3 first days of curing.

3.5 Robustness of sodium silicate-activated slag (NaS-slag)

The sodium silicate-activated slag mortar (w/b = 0.40, 20°C) had a compressive strength of 9.5 MPa to 77.8 MPa between 1 and 90 days. Figure 4 shows that early age mechanical strengths of NaS-slag mortar were more dependent on water content and temperature than those of CEM I mortar. For mixes containing less water (-5%) or cast and cured at high temperature (30°C) for 3 days, strong increases in mechanical strengths, respectively of +117% (20.6 MPa) and + 319% (39.1 MPa) were measured at 1 day, whereas, for mixes containing more water (+5%) and cast and cured at low temperature (10°C), a strong decrease was observed. At 10°C, the mechanical strengths were quite low at 1 and 2 days, only 1.3 MPa (-83%) and 2.3 MPa (-94%) respectively. NaS-slag and Geo mortars showed similar behaviour regarding temperature, but NaS-slag mortar showed more dependence on water content at the early age. At later ages (7, 28, and 90 days), neither the temperature of raw materials and curing temperature, nor the water content, seemed to have strong influence on compressive strengths in comparison to CEM I. The higher the water content, the lower the compressive strengths: 77.8 MPa, 80.6 MPa, and 73.0 MPa were respectively obtained at 90 days for mortar with w/b ratios of 0.40, 0.38, and 0.42. Hot casting and curing tended to limit final compressive strengths: 78.0 MPa, 77.8 MPa and 70.7 MPa were obtained at 90 days for 10°C, 20°C, and 30°C casting and curing respectively.

Longer curing times of 28 days and 90 days at 10°C yielded compressive strengths slightly lower than (28 days) or equivalent to (90 days) the reference NaS-slag mortar kept at 20°C: 68.9 MPa (-11%) and 79.6 MPa (+2%), respectively, which may be explained initially by a delay in hydration (see Figure 9).

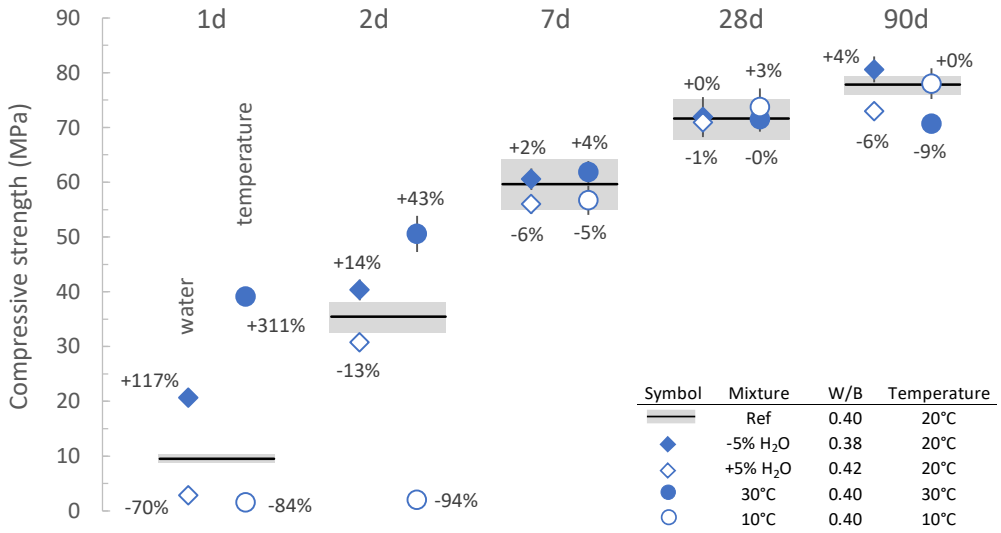

Figure 4: Evolution of compressive strengths in comparison to NaS-slag reference mortar depending on water content (±5%) and the temperature of raw materials at casting and during the 3 first days of curing.

3.6 Robustness of sodium metasilicate-activated slag (MS-slag)

The sodium metasilicate-activated slag mortar (w/b = 0.40, 20°C) had compressive strengths of 20.0 MPa to 62.0 MPa between 1 and 90 days. As for other mortars (CEM I, Geo, NaS-slag), the more water, the lower the compressive strengths, and inversely (adding 5% of water yielded -2% to -18 % between 1 and 90 days, without specific order). The early age properties were also strongly dependent on casting and curing temperatures: hot temperature (30°C) gave higher mechanical strengths at 1 day (+43%, 28.7 MPa) and 2 days (+12%, 34.2 MPa), while cold casting and curing temperature (10°C) resulted in a strong decrease in mechanical strengths at 1 day (-97%, 0.7 MPa), and 2 days (-89%, 3.2 MPa) (Figure 5). It was also noticed that using sodium silicate powders (metasilicates) instead of sodium silicate solutions (Betol 47 T), led to less sensitivity to water and temperature for early age properties (Figure 4 vs Figure 5). At later ages (7 days, 28 days, and 90 days), the mechanical strengths were very slightly impacted when the water content was increased or decreased by 5% and the temperature was set to 10°C or 30°C (Figure 5). A slight increase in mechanical strengths was measured for a sample containing less water (+6%, 45.9 MPa, and +8%, 56.9 MPa, at 7 and 28 days respectively), but a slight decrease of 4% was obtained at 90 days in comparison to reference sample with w/b ratio of 0.40, which fell within the confidence interval of 95%: ± 2.5 MPa at 90 days. For a sample containing 5% more water, a compressive strength decrease of 10% was measured at 90 days, which is comparable to CEM I, NaS-slag mortars. As regards samples cast and cured for three days at 10°C, +9% (47.2 MPa), +8%, (56.7 MPa) and +16% (71.8 MPa) were obtained at 7, 28, and 90 days, respectively. Samples cast and cured for three days at 30°C had generally lower long-term compressive strength, for example 56.4 MPa at 90 days (-9%).

Longer curing time times of 28 days and 90 days at 10°C yielded compressive strengths slightly higher than the strength of the reference MS-slag mortar kept at 20°C: 59.4 MPa (+12%) and 68.0 MPa (+10%), respectively (see Figure 9).

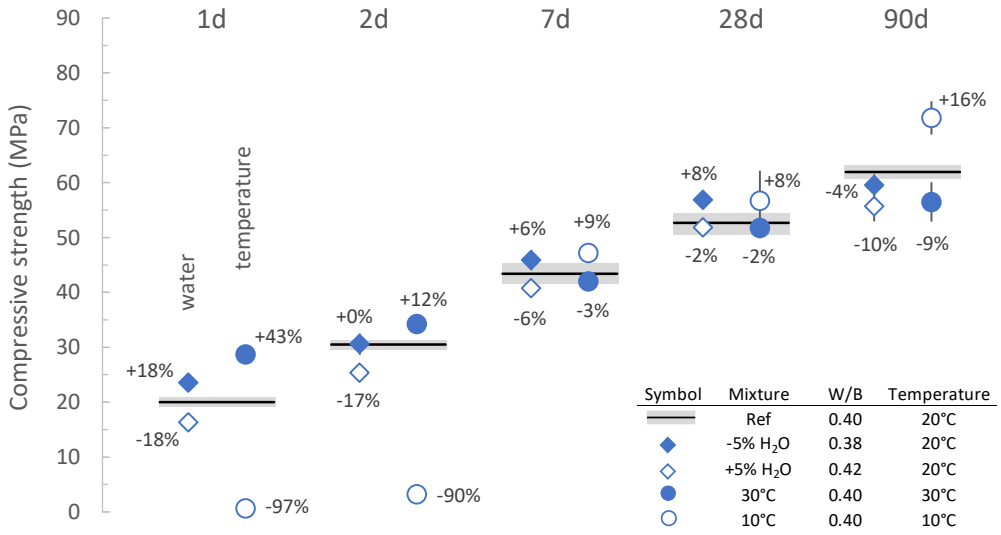

Figure 5: Evolution of compressive strengths in comparison to MS-slag reference mortar depending on water content (±5 %) and the temperature of raw materials and the 3 first days of curing.

3.7 Robustness of sodium carbonate-activated slag (NaC-slag)

The sodium carbonate-activated slag mortar (w/b = 0.40, 20°C) had a compressive strength of 0.8 MPa to 59.6 MPa from 1 to 90 days, respectively. As observed in Figure 6, sodium carbonate-activated slag mortar had limited early reactivity and it was, therefore, not possible to discuss the impact of water content or temperature variations on early compressive strengths. However, curing at 30°C significantly increased the reactivity and the strength development: 25.8 MPa was measured at 2 days compared to 1.3 MPa for the reference sample kept at 20°C. As previously observed for CEM I, Geo, NaS-slag, and MS-slag mortars, slight fluctuations were observed on 7-, 28- and 90-day mechanical strengths. At 28 days of curing, more water (+5%) or hot casting and curing (30°C) did not have much impact on compressive strengths (47.0 MPa and 45.3 MPa respectively); a decrease of 11% (41.4 MPa) was measured for cold casting and curing (10°C). At 90 days, the results were slightly different, more water or hot casting and curing led to small decreases of 7% (55.2 MPa) and 8% (54.9 MPa), respectively, and a decrease of 6% (56.3 MPa) was observed for cold casting and curing.

Longer curing times of 28 days and 90 days at 10°C yielded compressive strengths of 42.0 MPa and 61.3 MPa respectively, 10% lower (28 days) and 4% higher (90 days) than for the reference NaC-slag mortar kept 28 days at 20°C (see Figure 9). As for NaS-slag, cold curing that might be encountered during winter may delay hydration.

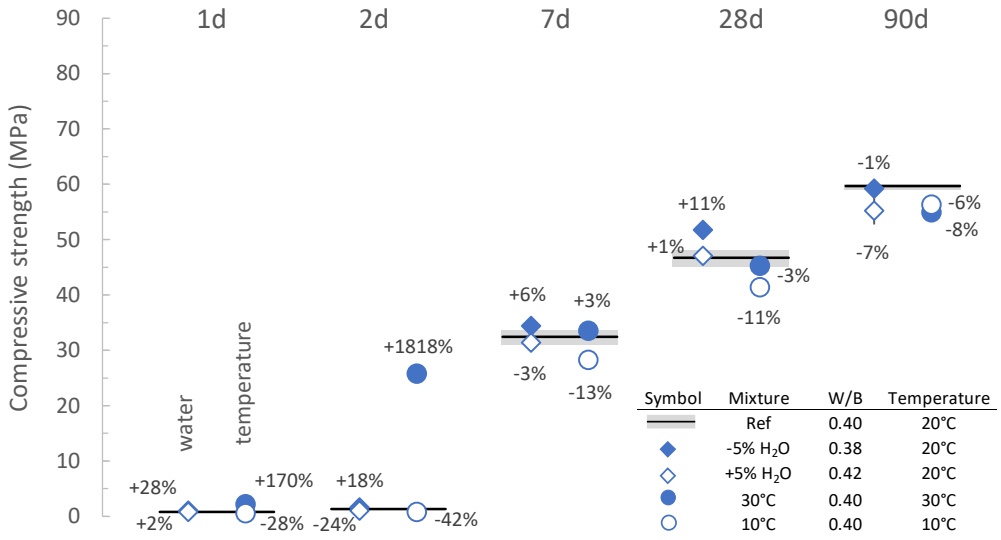

Figure 6: Evolution of compressive strengths in comparison to NaC-slag reference mortar depending on water content (±5%) and the temperature of raw materials and the 3 first days of curing.

3.8 Reaction/hydration heat and apparent activation energies for alkali-activated and CEM I pastes

The reaction heat of the five pastes over time was calculated from the integration of heat flux measurements at 12°C, 20°C and 30°C. This method is often used to characterize the kinetics of reaction and it provides a good picture of the amount of reaction products, such as hydrates in the case of cements [39]. The heat flux measurements and reaction/hydration heat release are presented in Figure 7 for each binder and the three temperatures studied.

For cement and slags (CEM I, NaS-slag, MS-slag, NaC-slag), the heat flux evolved according to three stages. The sharp instantaneous peak due to isothermal calorimeter equilibration after inserting the sample was not taken into account (30 to 45 minutes). First, the released heat was weak (latent period). This was followed by the period of acceleration indicating the formation of hydrates (mainly C-S-H for CEM I or C-A-S-H for alkali-activated binders). Finally, a period of deceleration resulted from the diffusion of water and ions through the layers of hydrates, which become increasingly thick [43], [52]. In the case of NaC-slag, two exothermic peaks were observed, suggesting two hydration products: $CaCO_3$ polymorphs (calcite, gaylussite) and C-A-S-H hydrates [59].

As regards the geopolymer binder (Geo), only a strong exothermic peak was observed at the beginning. The reaction started immediately after the mixing and it was therefore difficult to observe this early peak and accurately quantify the hydration heat after excluding the first 30 minutes.

For all five binders, it was noticed that increasing the temperature considerably accelerated the reactions (sharper and earlier exothermic peaks). The hydration/reaction heat evolutions clearly point out that the delay between 20°C and 12°C was greater than between 30°C and 20°C. This is in accordance with the drop of compressive strengths observed at early age on all mortars cured at 10°C. Furthermore, the mortars could also be classified by their final heat of reaction/hydration as follows:

- At 20°C and 30°C, Q_∞(CEM I) > Q_∞(Geo) > Q_∞(NaS-slag) and Q_∞(MS-slag) > Q_∞(NaC-slag),
- At 10°C, Q_∞(Geo) > Q_∞(CEM I) > Q_∞(NaS-slag) and Q_∞(MS-slag) > Q_∞(NaC-slag).

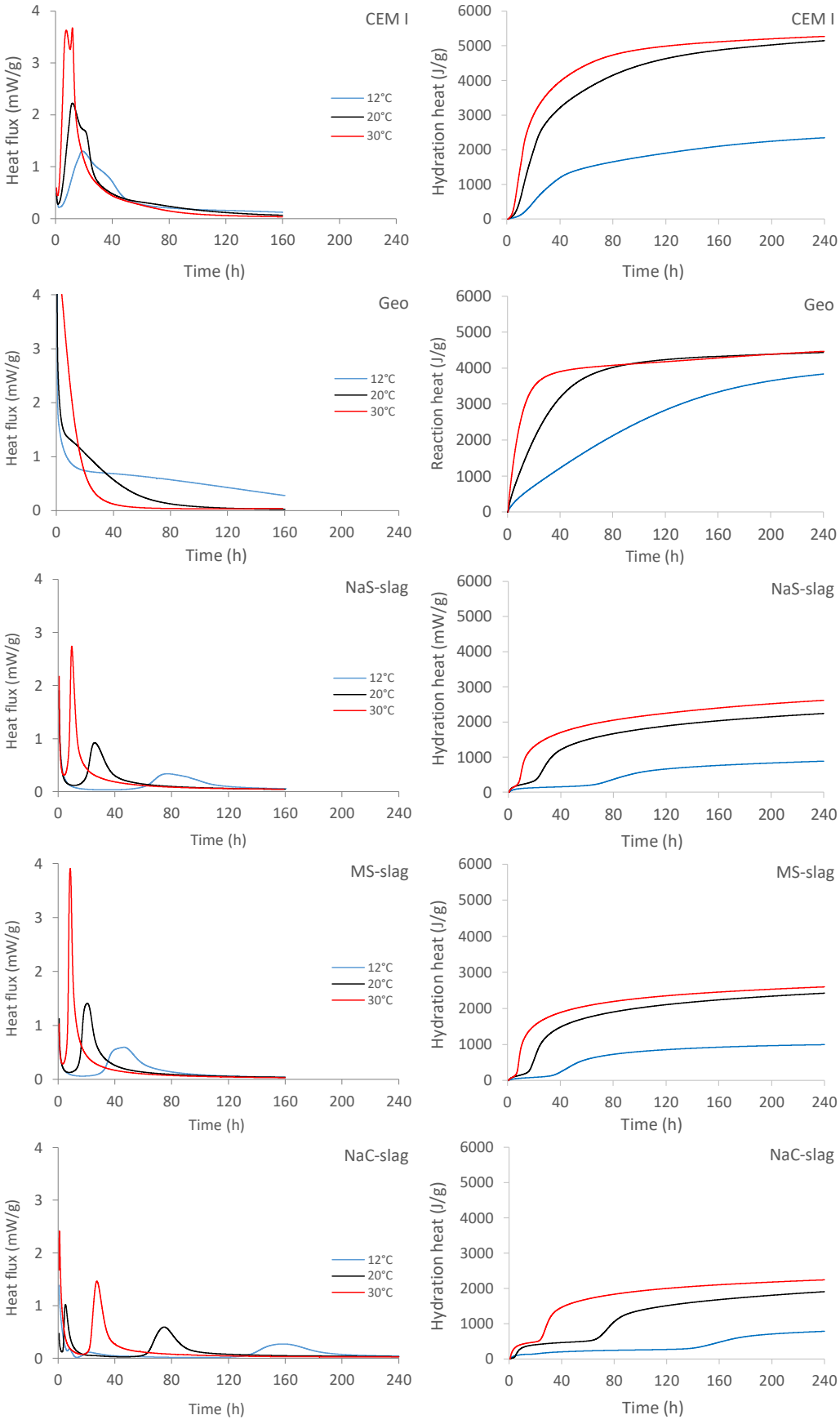

Figure 7: Evolution of the heat flux and heat of reaction/hydration over time for the five pastes studied.

From the hydration/reaction heat release, the apparent activation energies (E_a) could be determined on the five pastes depending on the degree of reaction/hydration (α, Eq. 2). The corresponding times to reach a given degree of reaction α (α = 0.2, α = 0.3, α = 0.4, α = 0.5, α = 0.6) were identified for each temperature (12°C, 20°C, 30°C) and then the apparent activation energies were obtained by plotting $-\ln(1/t_\alpha)$ against $(1/RT)$ and determining the slope of the linear relationship according to Eq. 5 (Figure 8-a for CEM I paste). The maximum degree of reaction was 0.6 because the measurements were only performed for 10 days. The results are presented in Figure 8-b and the time values identified for each temperature at the five degrees of reaction/hydration are given in Table 5.

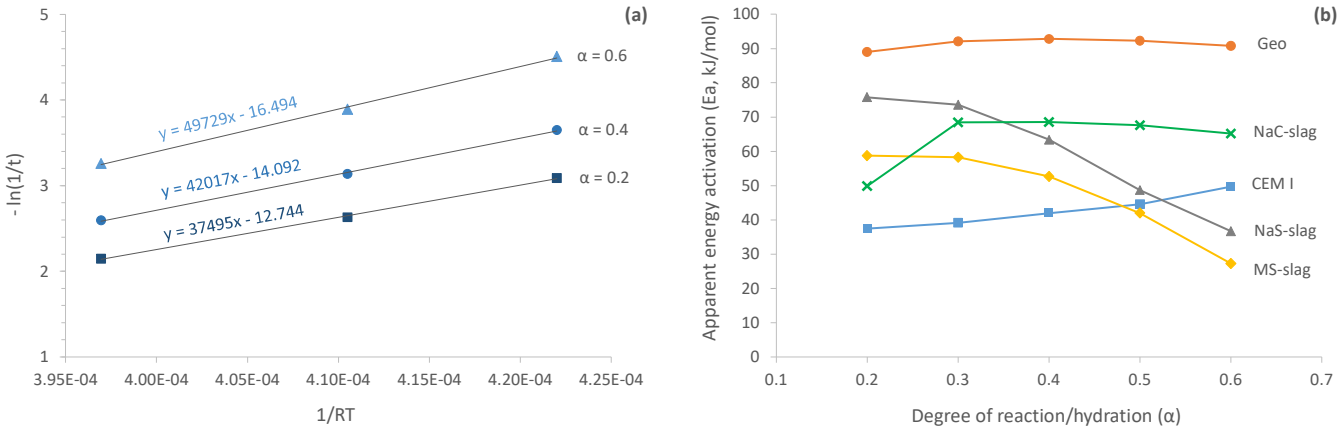

Figure 8: Arrhenius plot, showing –ln(1/t) against 1/RT for CEM I (a), and apparent activation energies for the five pastes studied (CEM I, Geo, NaS-slag, MS-slag, NaC-slag) depending on the degree of reaction/hydration (b).

Figure 8 and Table 5 show that apparent activation energies could vary depending on the degree of reaction selected. For CEM I paste, the apparent activation energy increased with the degree of hydration (37.5 kJ/mol for α = 0.2, 42.0 kJ/mol for α = 0.4, 49.7 kJ/mol for α = 0.6, Figure 8-a). That was probably why apparent activation energies between 32 kJ/mol and 46 kJ/mol have been reported in the literature for Portland cement depending on the authors [34]–[36], [39]. It was also reported that, according to the calculation method used, different values of apparent activation energies could be obtained: the value of instantaneous activation energy could increase by 20 kJ/mol in comparison with the evolution of the energy activation determined from parallel measurements at different temperatures [40]. Kada-Benameur et al. [39] found E_a (10-20°C) and E_a (20-30°C) respectively equal to about 32 kJ/mol and 38 kJ/mol and said that, generally, for CEM I, the apparent activation energy remains appreciably constant between α = 0.1 and α = 0.5. The variations at very young age (α ≤ 0.05) can be explained by the fact that the reaction is directed more by a diffusion mode. Moreover, in the long term (α > 0.5), we pass from a mode controlled by chemical reactions to a mode controlled by the diffusion of water through the layers of hydrates [39].

As regards alkali-activated binders, different behaviours were observed: the apparent activation energy of geopolymer binder (Geo) seemed rather constant over the whole range of degrees of reaction, while the apparent activation energies of slag activated binders (MS-slag, NaS-slag, NaC-slag) were more dependent on the degree of hydration (Figure 8-b). The apparent activation decreased significantly for MS-slag and NaS-slag when α > 0.4, and increased for NaC-slag when α > 0.2. This difference might be due to a difference in reactivity, since the reactivity is lower for NaC-slag. Thus, apparent activation energies of 89.0 kJ/mol (α = 0.2) and 92.3 kJ/mol (α = 0.5), 75.7 kJ/mol

(α = 0.2) and 48.7 kJ/mol (α = 0.5), 58.7 kJ/mol (α = 0.2) and 42 kJ/mol (α = 0.5), 49.9 kJ/mol (α = 0.2) and 67.6 kJ/mol (α = 0.5) could be determined for Geo, NaS-slag, MS-slag, and NaC-slag respectively. Some of these values are close to the ones reported in the literature: 84 kJ/mol for sodium metakaolin-based geopolymer [44], and 53.6 kJ/mol (α = 0.5) [43], 57.6 kJ/mol (α = 0.5) [42] for sodium silicate-activated slag (4% Na_2O). No value has been reported in the literature for NaC-slag systems so far.

It was noticed that alkali-activated materials had higher apparent activation energies than CEM I (37.5 kJ/mol for α = 0.2), this observation might explain why they seemed more dependent on temperature conditions at early age. Furthermore, according to apparent activation energy values, the geopolymer paste would be more dependent on temperature conditions than slag-activated materials would, and NaS-slag paste would be more sensitive than NaC-slag paste, which, itself, would be more sensitive than MS-slag paste.

Table 5: Time taken to reach 3 values of degree of reaction/hydration (α = 0.2, α = 0.4, α = 0.6) and the corresponding apparent activation energies for the five pastes (CEM I, Geo, NaS-slag, MS-slag, NaC-slag).

	CEM I				
α	0.2	0.3	0.4	0.5	0.6
t[10°C] (h)	22.0	29.3	38.5	55.3	90.7
t[20°C] (h)	13.9	18.2	23.0	32.1	49.0
t[30°C] (h)	8.6	11.0	13.4	18.1	26.0
Ea (kJ/mol)	37.5	39.5	42.0	44.6	49.7
	Geo				
α	0.2	0.3	0.4	0.5	0.6
t[10°C] (h)	28.4	47.5	68.0	94.0	118.1
t[20°C] (h)	8.2	13.4	19.3	26.2	34.8
t[30°C] (h)	3.0	4.7	6.6	8.9	12.0
Ea (kJ/mol)	89.0	92.1	92.8	92.3	90.8
	NaS-slag				
α	0.2	0.3	0.4	0.5	0.6
t[10°C] (h)	69.1	80.0	91.3	108.4	146.3
t[20°C] (h)	29.0	29.3	35.6	49.5	77.3
t[30°C] (h)	10.3	12.5	18.4	31.6	57.6
Ea (kJ/mol)	75.8	73.6	63.4	48.7	36.7
	MS-slag				
α	0.2	0.3	0.4	0.5	0.6
t[10°C] (h)	38.3	43.4	48.1	53.4	61.6
t[20°C] (h)	20.1	23.1	27.9	37.8	58.3
t[30°C] (h)	8.8	10.1	12.9	18.8	31.5
Ea (kJ/mol)	58.8	58.3	52.8	42	27.3
	NaC-slag				
α	0.2	0.3	0.4	0.5	0.6
t[10°C] (h)	71.8	147.8	160.5	174.4	205.1
t[20°C] (h)	61.2	753.0	79.4	91.1	127.4
t[30°C] (h)	21.0	26.5	28.9	32.3	40.6
Ea (kJ/mol)	49.9	68.5	68.6	67.6	65.2

4 Summary and discussion

4.1 Influence of water on the robustness of the five mortars

The results in this article on the influence of water content (± 5% H_2O) show that alkali-activated materials (Geo, NaS-Slag, MS-slag, NaC-slag) generally present levels of sensitivity to variations of water content that are similar to those of CEM I. Reducing water content by 5% caused a lower slump (Table 4) and higher compressive strengths, while adding 5% of water led to a greater slump (Table 4) and lower early compressive strengths. The early age properties were affected in the same way, except for the one-day compressive strength of sodium silicate-activated slag materials (NaS-slag), which had very different mechanical strengths depending on the w/b ratio (Figure 4). For this formulation, compressive strengths of 20.6 MPa, 9.5 MPa, and 2.8 MPa were measured for mortars with w/b equal to 0.38, 0.40, and 0.42, respectively. It is well known that adding or reducing water content delays or shortens hydration processes of cement, since the inter-particle spacing of cement grains is larger or smaller and more or less time is needed to reach supersaturation of hydrates [60], [61]. Additionally, in the case of alkali-activated materials, the activating solution is slightly diluted. For each material, the 28-day and 90-day mechanical strengths (final properties for CEM I and Geo) were not significantly changed by modifying the water content by 5%. CEM I mortar had the highest variations when water content increased: -13% at 28 days and -17 % at 90 days. This could have been due to the higher w/b ratio used to enable the casting and vibration of mortar bars (w/b = 0.5).

4.2 Influence of temperature on the robustness of the five mortars

The results in this article on the influence of raw material temperature and three days' curing temperature revealed that alkali-activated materials (Geo, NaS-Slag, MS-slag, NaC-slag) and CEM I had the same behaviour with regard to strength development. For high temperatures such as could be encountered during summer (30°C), a gain of mechanical strengths was observed at early age, which could be attributed to an acceleration in hydration/geopolymerization processes. In the case of alkali-activated binders, this could be explained by an increase in the solubility of activators (Na_2CO_3 [55] and silica species [62], [63]), implying an increase in pH value that might speed up the dissolution of raw materials, hydration, and compressive strength development. For cold temperatures that could be encountered during winter (10°C), a loss of mechanical strength was observed in the early age, which could be attributed to a delay in hydration/geopolymerization processes. These observations had already been highlighted by several authors for CEM I [56]–[58], [64]–[66], metakaolin-based geopolymer [28], [67], [68] and alkali-activated slag materials [27], [69], [70].

However, early age properties seemed more dependent on temperature in all alkali-activated materials than in CEM I especially in cases of cold casting and curing. For CEM I mortars kept at 10°C for three days of curing, a drop in compressive strengths of 66% (at 1 day) and 42% (at day 2) were measured in comparison to the reference sample kept at 20°C during curing (Figure 2). In the case of alkali-activated materials, with the exception of the NaC-slag mix which cannot be discussed here because of its low reactivity (Figure 6), the drop measured in mechanical strengths was always greater than 80 % at 1 and 2 days. For instance, the compressive strength of geopolymer mortar could not be measured at 1 day, since it was still in the plastic stage and not completely set (taken as 0 MPa instead of the 38.9 MPa of the reference sample in Figure 3). The compressive strengths of metasilicate-activated slag materials were also really low at 1 day, 0.7 MPa instead of 20 MPa (Figure

5). The lower compressive strengths at 10°C for alkali-activated binders might be explained by their higher apparent activation energy: the reactions were slower and more energy was needed to enable rapid strength development.

Whatever the temperature of raw materials (liquids + powders + sand) and the first 3 days of curing (10°C, 20°C, 30°C), the 28-day compressive strengths were not significantly affected for any of the materials. However, in the longer term (90 days), samples cured at lower temperature (10°C) tended to attain better performances than samples initially cured at high temperature (30°C). Moreover, longer curing at 10°C (28 days and 90 days) yielded higher compressive strengths for CEM I at both maturing times (+22% and +15%), and slightly lower (except for MS-slag) and higher (except for Geo) compressive strengths for alkali-activated mortars at 28 days and 90 days respectively (Figure 9). These observations may have been due to a delay of the reaction/hydration induced by cold curing. In the case of geopolymer and sodium silicate-activated slag, the variations were small and fell within the confidence interval of 95%.

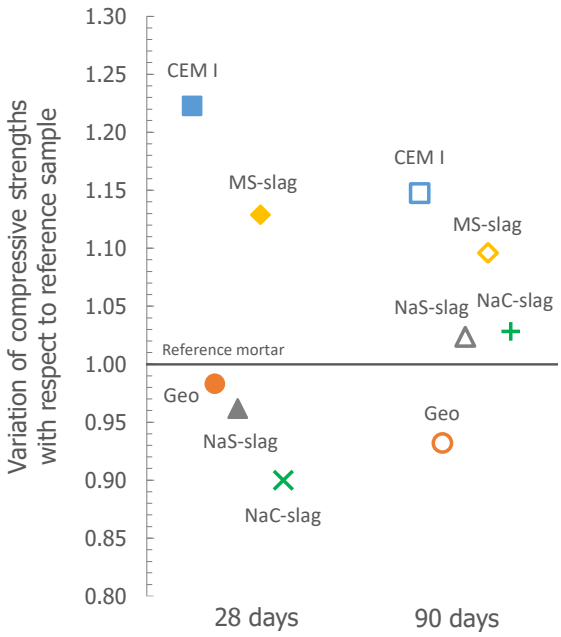

Figure 9: Variations of compressive strengths between samples kept for 28 days and 90 days at 20°C (reference mortars) and 10°C for the five mortars studied (CEM I, Geo, NaS-slag, MS-slag, NaC-slag).

As regards the effect of temperature of the raw materials on slump (Table 4), the alkali-activated materials also seemed more dependent than CEM I. Nevertheless, it should be noted that the CEM I employed in this study presented a low slump in classical casting conditions of mortar. The slump differences observed between the four alkali-activated materials mainly depended on the nature of the activator. The fact that Na_2CO_3 is hygroscopic (wetting agent) and its solubility increases with temperature [55] might explain why a higher slump was measured for raw materials kept at 30°C. In the case of mixes containing silica species (NaS-slag, MS-slag, Geo), it is also known that such species are more soluble at higher temperature and the sodium silicate solutions are less viscous [62], [63]. However, in contrast to sodium carbonate-activated slag mix (NaC-slag), lower and higher slumps were measured for mixes cast with raw materials kept at 30°C and 10°C, respectively. The loss of workability at higher temperature (30°C), especially for sodium silicate-activated slag mixes (MS-slag, NaS-slag), could be explained by a faster reaction and setting in comparison with the NaC-slag mix. The better workability at lower temperature (10°C) in presence of silica species in solution might be

caused by very slow hydration processes (slow dissolution of raw materials and slow precipitation of hydrates consuming water). It has been observed previously on conventional calcium silicate cement that slump increased and the water demand decreased during cold weather [71]–[73].

5 Conclusion

This paper has reported slump and compressive strength results for five mortars (CEM I, Geo, NaS-slag, MS-slag, NaC-slag) depending on the conditions that might be encountered for precasting or in situ concreting: variations of water content (± 5 %) and temperature (10°C, 20°C, 30°C). The aim was to evaluate the robustness of four alkali-activated mortars in accordance with these parameters, then compare them to an ordinary Portland cement mortar (CEM I). The results showed that:

- the metakaolin-based geopolymer, the sodium silicate-activated slag, the sodium metasilicate-activated slag, and the sodium carbonate-activated slag were as robust as an ordinary Portland cement (CEM I) in the long term. The 28-day and 90-day compressive strengths did not seem to be any more affected by slight fluctuations in water content and casting and curing temperature than those of CEM I did.
- they could be used instead of Portland cement for precasting or in situ concreting for temperatures above 20°C. However, during cold weather, their early age properties appeared to be more affected than CEM I. Thus, they could prove tricky to use during winter if preventive measures, such as the use of hot water, significant water to binder ratio reduction or even mix design modifications, were not set up.
- alkali-activated binders had higher apparent activation energy than CEM I: 89.0 kJ/mol (α =0.2) and 92.3 kJ/mol (α = 0.5), 75.7 kJ/mol (α = 0.2) and 48.7 kJ/mol (α = 0.5), 58.7 kJ/mol (α = 0.2) and 42 kJ/mol (α = 0.5), 49.9 kJ/mol (α = 0.2) and 67.6 kJ/mol (α = 0.5) were respectively found for the metakaolin-based geopolymer, the sodium silicate-activated slag, the sodium metasilicate-activated slag, and the sodium carbonate-activated slag. This can explain their higher sensitivity to temperature variations. Therefore, hot curing might have an interest for alkali-activated materials.

6 Acknowledgement

This work was supported by the L2A project funded by EDF, VINCI CONSTRUCTION, VICAT, ARGECO DEVELOPPEMENT, ECOCEM, and MBCC Group.

7 References

[1] J. L. Provis, “Alkali-activated materials,” *Rep. UNEP SBCI Work. GROUP LOW-CO2 ECO-Effic. Cem.-BASED Mater.*, vol. 114, pp. 40–48, Dec. 2018, doi: 10.1016/j.cemconres.2017.02.009.

[2] C. Shi, P. V. Krivenko, and D. M. Roy, *Alkali-Activated Cements and Concrete*. London and New York: Taylor & Francis, 2006.

[3] T. Glasby, J. Day, R. Genrich, and J. Aldred, “EFC Geopolymer Concrete Aircraft Pavements at Brisbane West Wellcamp Airport,” *Concr. 2015 27th Bienn. Natl. Conf. Concr. Inst. Aust. Conjunction 69th RILEM Week*, pp. 1051–1059, Melbourne, Australia 2015.

[4] P. V. Krivenko, *Alkaline Cements and Concretes: Proceedings of the First International Conference Held at the Scientific-Research Institute on Binders and Materials Named After V. D. Glukhovsky, Kiev, Ukraine on 11 -14 October 1994*. VIPOL Stock Company, 1994.

[5] J. L. Provis *et al.*, “Demonstration projects and applications in building and civil infrastructure,” in *Alkali-Activated Materials: State-of-the-Art Report, RILEM TC 224-AAM*, Springer/RILEM, 2014, pp. 309–338.
[6] K. Yang, C. Yang, J. Zhang, Q. Pan, L. Yu, and Y. Bai, “First structural use of site-cast, alkali-activated slag concrete in China,” *Proc. Inst. Civ. Eng. - Struct. Build.*, vol. 171, no. 10, pp. 800–809, 2018, doi: 10.1680/jstbu.16.00193.
[7] C. Li, H. Sun, and L. Li, “A review: The comparison between alkali-activated slag (Si+Ca) and metakaolin (Si+Al) cements,” *Cem. Concr. Res.*, vol. 40, no. 9, pp. 1341–1349, Sep. 2010, doi: 10.1016/j.cemconres.2010.03.020.
[8] A. Humad, K. Habermehl-Cwirzen, and A. Cwirzen, “Effects of fineness and chemical composition of blast furnace slag on properties of alkali-activated binder,” *Materials*, vol. 12, no. 20, 2019, doi: 10.3390/ma12203447.
[9] M. R. Rowles, J. V. Hanna, K. J. Pike, M. E. Smith, and B. H. O’Connor, “29Si, 27Al, 1H and 23Na MAS NMR Study of the Bonding Character in Aluminosilicate Inorganic Polymers,” *Appl. Magn. Reson.*, vol. 32, no. 4, p. 663, Dec. 2007, doi: 10.1007/s00723-007-0043-y.
[10] S. Park, S. Y. Abate, and H.-K. Kim, “Hydration kinetics modeling of sodium silicate-activated slag: A comparative study,” *Constr. Build. Mater.*, vol. 242, p. 118144, May 2020, doi: 10.1016/j.conbuildmat.2020.118144.
[11] R. J. Myers, S. A. Bernal, and J. L. Provis, “Phase diagrams for alkali-activated slag binders,” *Cem. Concr. Res.*, vol. 95, pp. 30–38, May 2017, doi: 10.1016/j.cemconres.2017.02.006.
[12] H. Ye and A. Radlińska, “Quantitative Analysis of Phase Assemblage and Chemical Shrinkage of Alkali-Activated Slag,” *J. Adv. Concr. Technol.*, vol. 14, pp. 245–260, May 2016, doi: 10.3151/jact.14.245.
[13] S. A. Bernal, J. L. Provis, R. J. Myers, R. San Nicolas, and J. S. J. van Deventer, “Role of carbonates in the chemical evolution of sodium carbonate-activated slag binders,” *Mater. Struct.*, vol. 48, no. 3, pp. 517–529, Mar. 2015, doi: 10.1617/s11527-014-0412-6.
[14] P. Awoyera and A. Adesina, “A critical review on application of alkali activated slag as a sustainable composite binder,” *Case Stud. Constr. Mater.*, vol. 11, p. e00268, Dec. 2019, doi: 10.1016/j.cscm.2019.e00268.
[15] J. L. Provis *et al.*, “RILEM TC 247-DTA round robin test: mix design and reproducibility of compressive strength of alkali-activated concretes,” *Mater. Struct.*, vol. 52, no. 5, p. 99, Sep. 2019, doi: 10.1617/s11527-019-1396-z.
[16] T. Luukkonen, Z. Abdollahnejad, J. Yliniemi, P. Kinnunen, and M. Illikainen, “One-part alkali-activated materials: A review,” *Cem. Concr. Res.*, vol. 103, pp. 21–34, Jan. 2018, doi: 10.1016/j.cemconres.2017.10.001.
[17] L. S.-C. Ko *et al.*, “AAM Concretes: Standards for Mix Design/Formulation and Early-Age Properties,” in *Alkali Activated Materials: State-of-the-Art Report, RILEM TC 224-AAM*, J. L. Provis and J. S. J. van Deventer, Eds. Dordrecht: Springer Netherlands, 2014, pp. 157–176.
[18] C. Ruiz-Santaquiteria, J. Skibsted, A. Fernández-Jiménez, and A. Palomo, “Alkaline solution/binder ratio as a determining factor in the alkaline activation of aluminosilicates,” *Cem. Concr. Res.*, vol. 42, no. 9, pp. 1242–1251, Sep. 2012, doi: 10.1016/j.cemconres.2012.05.019.
[19] A. Niş, “Compressive strength variation of alkali activated fly ash/slag concrete with different NaOH concentrations and sodium silicate to sodium hydroxide ratios,” *J. Sustain. Constr. Mater. Technol.*, vol. 4, pp. 351–360, Oct. 2019, doi: 10.29187/jscmt.2019.39.
[20] S. Fang, E. S. S. Lam, B. Li, and B. Wu, “Effect of alkali contents, moduli and curing time on engineering properties of alkali activated slag,” *Constr. Build. Mater.*, vol. 249, p. 118799, Jul. 2020, doi: 10.1016/j.conbuildmat.2020.118799.
[21] K. Wianglor, S. Sinthupinyo, M. Piyaworapaiboon, and A. Chaipanich, “Effect of alkali-activated metakaolin cement on compressive strength of mortars,” *Appl. Clay Sci.*, vol. 141, pp. 272–279, Jun. 2017, doi: 10.1016/j.clay.2017.01.025.

[22] S. A. Bernal, “Effect of the activator dose on the compressive strength and accelerated carbonation resistance of alkali silicate-activated slag/metakaolin blended materials,” *Constr. Build. Mater.*, vol. 98, pp. 217–226, Nov. 2015, doi: 10.1016/j.conbuildmat.2015.08.013.
[23] M. R. Karim, M. M. Hossain, M. Manjur A Elahi, and M. F. Mohd Zain, “Effects of source materials, fineness and curing methods on the strength development of alkali-activated binder,” *J. Build. Eng.*, vol. 29, p. 101147, May 2020, doi: 10.1016/j.jobe.2019.101147.
[24] G. Samson, M. Cyr, and X. X. Gao, “Formulation and characterization of blended alkali-activated materials based on flash-calcined metakaolin, fly ash and GGBS,” *Construction and Building Materials*, pp. 50–64, 2017.
[25] A. Adam, S. Maricar, and B. Ramadhan, “The Effects of Water to Solid Ratio, Activator to Binder Ratio, and Lime Proportion on the Compressive Strength of Ambient-Cured Geopolymer Concrete,” May 2019, doi: 10.22146/jcef.43878.
[26] K.-H. Yang, A.-R. Cho, and J.-K. Song, “Effect of water–binder ratio on the mechanical properties of calcium hydroxide-based alkali-activated slag concrete,” *Constr. Build. Mater.*, vol. 29, pp. 504–511, Apr. 2012, doi: 10.1016/j.conbuildmat.2011.10.062.
[27] T. Medina, S. Arredondo-Rea, J. Gómez-Soberón, C. Rosas, and R. Corral Higuera, “EFFECT OF CURING TEMPERATURE IN THE ALKALI-ACTIVATED BLAST-FURNACE SLAG PASTE AND THEIR STRUCTURAL INFLUENCE OF POROSITY,” *Adv. Sci. Technol. Res. J.*, vol. 10, pp. 74–79, Sep. 2016, doi: 10.12913/22998624/64021.
[28] J. Yuan *et al.*, “Effect of curing temperature and SiO2/K2O molar ratio on the performance of metakaolin-based geopolymers,” *Ceram. Int.*, vol. 42, no. 14, pp. 16184–16190, Nov. 2016, doi: 10.1016/j.ceramint.2016.07.139.
[29] Z. Kubba *et al.*, “Impact of curing temperatures and alkaline activators on compressive strength and porosity of ternary blended geopolymer mortars,” *Case Stud. Constr. Mater.*, vol. 9, p. e00205, Dec. 2018, doi: 10.1016/j.cscm.2018.e00205.
[30] F. N. Okoye, J. Durgaprasad, and N. B. Singh, “Mechanical properties of alkali activated flyash/Kaolin based geopolymer concrete,” *Constr. Build. Mater.*, vol. 98, pp. 685–691, Nov. 2015, doi: 10.1016/j.conbuildmat.2015.08.009.
[31] P. Shoaei, H. R. Musaeei, F. Mirlohi, S. Narimani zamanabadi, F. Ameri, and N. Bahrami, “Waste ceramic powder-based geopolymer mortars: Effect of curing temperature and alkaline solution-to-binder ratio,” *Constr. Build. Mater.*, vol. 227, p. 116686, Dec. 2019, doi: 10.1016/j.conbuildmat.2019.116686.
[32] B. Bosiljkov V, K. Fijavž M, and M. Serdar, “Mechanical properties of cement based materials—extended round robin test of COST Action TU 1404,” *Azenha M Schlicke Benboudjema F Jedrzejewska Eds Proc. SynerCrete’18 Int. Conf. Interdiscip. Approaches Cem.-Based Mater. Struct. Concr.*, vol. Funchal, Portugal, RILEM proceedings PRO121, pp. 47–54, 2018.
[33] K. Ezziane, A. Bougara, A. Kadri, H. Khelafi, and E. Kadri, “Compressive strength of mortar containing natural pozzolan under various curing temperature,” *Cem. Concr. Compos.*, vol. 29, no. 8, pp. 587–593, Sep. 2007, doi: 10.1016/j.cemconcomp.2007.03.002.
[34] D. M. Roy and G. M. ldorn, “Hydration, Structure, and Properties of Blast Furnace Slag Cements, Mortars, and Concrete,” *ACI J. Proc.*, vol. 79, no. 6, Jan. 1982, doi: 10.14359/10919.
[35] Anton K. Schindler, “Effect of Temperature on Hydration of Cementitious Materials,” *ACI Mater. J.*, vol. 101, no. 1, Jan. 2004, doi: 10.14359/12990.
[36] W. Ma, D. Sample, R. Martin, and P. Brown, “Calorimetric Study of Cement Blends Containing Fly Ash, Silica Fume, and Slag at Elevated Temperatures,” *Cem. Concr. Aggreg.*, vol. 16, no. 2, pp. 93–99, Dec. 1994, doi: 10.1520/CCA10285J.
[37] X. Wu, D. M. Roy, and C. A. Langton, “Early stage hydration of slag-cement,” *Cem. Concr. Res.*, vol. 13, no. 2, pp. 277–286, Mar. 1983, doi: 10.1016/0008-8846(83)90111-4.
[38] X.-Y. Wang and H.-S. Lee, “Heat of hydration models of cementitious materials,” *Adv. Cem. Res.*, vol. 24, no. 2, pp. 77–90, 2012, doi: 10.1680/adcr.11.00007.

[39] H. Kada-Benameur, E. Wirquin, and B. Duthoit, “Determination of apparent activation energy of concrete by isothermal calorimetry,” *Cem. Concr. Res.*, vol. 30, no. 2, pp. 301–305, Feb. 2000, doi: 10.1016/S0008-8846(99)00250-1.
[40] S. Joseph, S. Uppalapati, and O. Cizer, “Instantaneous activation energy of alkali activated materials,” *RILEM Tech. Lett.*, vol. 3, pp. 121–123, Mar. 2019, doi: 10.21809/rilemtechlett.2018.78.
[41] H. Mehdizadeh and E. Najafi Kani, “Rheology and apparent activation energy of alkali activated phosphorous slag,” *Constr. Build. Mater.*, vol. 171, pp. 197–204, May 2018, doi: 10.1016/j.conbuildmat.2018.03.130.
[42] A. Fernández-Jiménez and F. Puertas, “Alkali-activated slag cements: Kinetic studies,” *Cem. Concr. Res.*, vol. 27, pp. 359–368, 1997.
[43] Z. Huanhai, W. Xue-quan, X. Zhongzi, and T. Ming-shu, “Kinetic study on hydration of alkali-activated slag,” *Cem. Concr. Res.*, vol. 23, pp. 1253–1258, 1993.
[44] H. Rahier, J. Wastiels, M. Biesemans, R. Willlem, G. Van Assche, and B. Van Mele, “Reaction mechanism, kinetics and high temperature transformations of geopolymers,” *J. Mater. Sci.*, vol. 42, no. 9, pp. 2982–2996, May 2007, doi: 10.1007/s10853-006-0568-8.
[45] C. E. White, J. L. Provis, B. Bloomer, N. J. Henson, and K. Page, “In situ X-ray pair distribution function analysis of geopolymer gel nanostructure formation kinetics,” *Phys Chem Chem Phys*, vol. 15, no. 22, pp. 8573–8582, 2013, doi: 10.1039/C3CP44342F.
[46] E. Najafi Kani, A. Allahverdi, and J. L. Provis, “Calorimetric study of geopolymer binders based on natural pozzolan,” *J. Therm. Anal. Calorim.*, vol. 127, no. 3, pp. 2181–2190, Mar. 2017, doi: 10.1007/s10973-016-5850-7.
[47] A. Poulesquen, F. Frizon, and D. Lambertin, “Rheological Behavior of Alkali-Activated Metakaolin During Geopolymerization,” in *Cement-Based Materials for Nuclear Waste Storage*, F. Bart, C. Cau-di-Coumes, F. Frizon, and S. Lorente, Eds. New York, NY: Springer New York, 2013, pp. 225–238.
[48] M. L. Granizo and M. T. Blanco, “Alkaline Activation of Metakaolin An Isothermal Conduction Calorimetry Study,” *J. Therm. Anal. Calorim.*, vol. 52, no. 3, pp. 957–965, Jun. 1998, doi: 10.1023/A:1010176321136.
[49] M. L. Granizo, M. T. Blanco-Varela, and A. Palomo, “Influence of the starting kaolin on alkali-activated materials based on metakaolin. Study of the reaction parameters by isothermal conduction calorimetry,” *J. Mater. Sci.*, vol. 35, no. 24, pp. 6309–6315, Dec. 2000, doi: 10.1023/A:1026790924882.
[50] X. Yao, Z. Zhang, H. Zhu, and Y. Chen, “Geopolymerization process of alkali–metakaolinite characterized by isothermal calorimetry,” *Thermochim. Acta*, vol. 493, no. 1, pp. 49–54, Sep. 2009, doi: 10.1016/j.tca.2009.04.002.
[51] Z. Sun and A. Vollpracht, “Isothermal calorimetry and in-situ XRD study of the NaOH activated fly ash, metakaolin and slag,” *Cem. Concr. Res.*, vol. 103, pp. 110–122, Jan. 2018, doi: 10.1016/j.cemconres.2017.10.004.
[52] C. Shi and R. L. Day, “A calorimetric study of early hydration of alkali-slag cements,” *Cem. Concr. Res.*, vol. 25, no. 6, pp. 1333–1346, Aug. 1995, doi: 10.1016/0008-8846(95)00126-W.
[53] D. Ravikumar and N. Neithalath, “Reaction kinetics in sodium silicate powder and liquid activated slag binders evaluated using isothermal calorimetry,” *Thermochim. Acta*, vol. 546, pp. 32–43, Oct. 2012, doi: 10.1016/j.tca.2012.07.010.
[54] B. J. Lee, J. W. Bang, K. J. Shin, and Y. Y. Kim, “The Effect of Specimen Size on the Results of Concrete Adiabatic Temperature Rise Test with Commercially Available Equipment,” *Mater. Basel Switz.*, vol. 7, no. 12, pp. 7861–7874, Dec. 2014, doi: 10.3390/ma7127861.
[55] R. C. Wells and D. J. McAdam, “PHASE RELATIONS OF THE SYSTEM: SODIUM CARBONATE AND WATER,” *J. Am. Chem. Soc.*, vol. 29, no. 5, pp. 721–727, May 1907, doi: 10.1021/ja01959a009.
[56] I. Elkhadiri, M. Palacios, and F. Puertas, “Effect of curing temperature on cement hydration.,” *Ceramics – Silikáty*, pp. 65–75, 2009.

[57] S. Martínez-Ramírez and M. Frías, “The effect of curing temperature on white cement hydration,” *Constr. Build. Mater.*, vol. 23, no. 3, pp. 1344–1348, Mar. 2009, doi: 10.1016/j.conbuildmat.2008.07.012.
[58] l ubomír Je\vzo, T. Ifka, B. Cvopa, JANKA \vSKUNDOVÁ, K. VLADIMÍR, and M. Palou, “EFFECT OF TEMPERATURE UPON THE STRENGTH DEVELOPMENT RATE AND UPON THE HYDRATION KINETICS OF CEMENTS,” 2010.
[59] X. Ke, S. A. Bernal, and J. L. Provis, “Controlling the reaction kinetics of sodium carbonate-activated slag cements using calcined layered double hydroxides,” *Cem. Concr. Res.*, vol. 81, pp. 24–37, Mar. 2016, doi: 10.1016/j.cemconres.2015.11.012.
[60] A. M. Ley-Hernandez, J. Lapeyre, R. Cook, A. Kumar, and D. Feys, “Elucidating the Effect of Water-To-Cement Ratio on the Hydration Mechanisms of Cement,” *ACS Omega*, vol. 3, no. 5, pp. 5092–5105, May 2018, doi: 10.1021/acsomega.8b00097.
[61] X. Pang, “The effect of water-to-cement ratio on the hydration kinetics of Portland cement at different temperatures,” *Conf. 14th Int. Congr. Cem. Chem. Beijing China*, Oct. 2015.
[62] G. B. Alexander, W. M. Heston, and R. K. Iler, “The Solubility of Amorphous Silica in Water,” *J. Phys. Chem.*, vol. 58, no. 6, pp. 453–455, Jun. 1954, doi: 10.1021/j150516a002.
[63] R. Siever, “Silica Solubility, 0°-200° C., and the Diagenesis of Siliceous Sediments,” *J. Geol.*, vol. 70, no. 2, pp. 127–150, 1962.
[64] B. Lothenbach, F. Winnefeld, C. Alder, E. Wieland, and P. Lunk, “Effect of temperature on the pore solution, microstructure and hydration products of Portland cement pastes,” *Cem. Concr. Res.*, vol. 37, no. 4, pp. 483–491, Apr. 2007, doi: 10.1016/j.cemconres.2006.11.016.
[65] B. Lothenbach, T. Matschei, G. Möschner, and F. P. Glasser, “Thermodynamic modelling of the effect of temperature on the hydration and porosity of Portland cement,” *Cem. Concr. Res.*, vol. 38, no. 1, pp. 1–18, Jan. 2008, doi: 10.1016/j.cemconres.2007.08.017.
[66] J. I. Escalante-Garcia and J. H. Sharp, “The effect of temperature on the early hydration of Portland cement and blended cements,” *Adv. Cem. Res.*, vol. 12, no. 3, pp. 121–130, Jul. 2000, doi: 10.1680/adcr.2000.12.3.121.
[67] M. S. Muñiz-Villarreal *et al.*, “The effect of temperature on the geopolymerization process of a metakaolin-based geopolymer,” *Mater. Lett.*, vol. 65, no. 6, pp. 995–998, Mar. 2011, doi: 10.1016/j.matlet.2010.12.049.
[68] B. Mo, H. Zhu, X. Cui, Y. He, and S. Gong, “Effect of curing temperature on geopolymerization of metakaolin-based geopolymers,” *Appl. Clay Sci.*, vol. 99, pp. 144–148, Sep. 2014, doi: 10.1016/j.clay.2014.06.024.
[69] Y. M. Gu, Y. H. Fang, Y. F. Gong, Y. R. Yan, and C. H. Zhu, “Effect of curing temperature on setting time, strength development and microstructure of alkali activated slag cement,” *Mater. Res. Innov.*, vol. 18, no. sup2, pp. S2-829, May 2014, doi: 10.1179/1432891714Z.000000000467.
[70] B. S. Gebregziabiher, R. J. Thomas, and S. Peethamparan, “Temperature and activator effect on early-age reaction kinetics of alkali-activated slag binders,” *Constr. Build. Mater.*, vol. 113, pp. 783–793, Jun. 2016, doi: 10.1016/j.conbuildmat.2016.03.098.
[71] A. Husain, J. Ahmad, A. Mujeeb, and R. Ahmed, “Effects of temperature on concrete,” *Int. J. Adv. Res. Sci. Eng. IJARSE*, vol. 05, no. 03, pp. 33–42, Mar. 2016.
[72] A. M. Neville, “Properties of Concrete - Chapter 8: Temperature effect on concrete,” 5th Edition., 2011.
[73] J. Bashir, S. Ahmad Rather, F. Ahmad Laherwal, and V. Garg, “Impact of cold weather on workability, compressive and flexural strength of concrete.,” *Int. Res. J. Eng. Technol. IRJET*, vol. 06, no. 12, pp. 643–646, Dec. 2019.